

A probabilistic description of the wind over Liverpool Bay with application to oil spill simulations

A.J. Elliott

Centre for Applied Marine Sciences, University of Wales, Bangor, Marine Science Laboratories, Menai Bridge, Anglesey LL59 5AB, UK

Received 23 February 2004; accepted 30 June 2004

Abstract

Surface winds from the UK Meteorological Office mesoscale (12 km grid) atmospheric model have been used to define the wind at a location in Liverpool Bay during 1997–2001. Winds from the SW (centred on 240°) with a speed of about 10 m/s (20 knots) were the most frequent, although weaker winds from the SE were also common. The wind spectra were red in character and showed no evidence for a peak at the synoptic (2–5 day) time scale; however, a zero-up-crossing analysis suggested a dominant periodicity at 3.1 days, and at this time scale the winds were spatially coherent over a distance of 300 km. A wind direction transition matrix was derived to quantify the probability with which the wind changed between two specified directions. This information was then used with an estimate of the mean duration of a wind event to compute a stochastic wind time series that contained a similar energy level, periodicity, and direction variability to the archived wind data. The archived and stochastic winds were then used in 1000 oil spill contingency simulations during which estimates of the mean and minimum times taken for oil to reach the coastline, and the percentage of the oil impacting selected sites were computed. The stochastic winds provided more realistic results, when compared against those derived using the wind archive, than those obtained using a wind rose representation of the winds. The derivation and use of a stochastic wind time series has application to a range of modelling studies.

© 2004 Elsevier Ltd. All rights reserved.

Keywords: synoptic winds; probability; transition; oil spill; contingency; Liverpool Bay; Irish Sea

1. Introduction

An essential element of oil spill preparedness is the assessment of risk for coastlines and nearshore waters that are considered to be vulnerable to damage by oil pollution. In the broadest sense this requires an evaluation of ship traffic and the likelihood of accidents within shipping corridors, as well as an assessment of the likelihood of releases from fixed offshore installations and the impact on the surrounding waters (Galt and Payton, 1999). The impact of the oil can then be evaluated in terms of both the quantity of oil reaching a

shoreline, and in terms of the exposure of the nearshore waters to oil pollution. This latter aspect is both a function of the concentration of oil in the water column and the length of time for which a region is affected. In addition, the time taken for oil to reach a location can have an influence on the quantity of oil that arrives at a beach and of the eventual toxicity of that oil on the environment. Contingency planning, therefore, should evaluate not only the probability that a region will be influenced by spilled oil, but should also assess the time taken for the oil to reach the location, as well as estimate the exposure of the region to oil.

In order to make oil spill contingency calculations it is necessary to have access either to a deterministic archive of recorded winds, or to make use of statistical

E-mail address: a.j.elliott@bangor.ac.uk.

descriptions of the wind field which have traditionally been provided by wind roses. The disadvantage of the wind rose is that it does not contain information on the time variability of the wind such as the duration of wind events and the probability of the transition between wind directions. However, these deficiencies can be remedied through the determination of the dominant time scales and the derivation of a direction transition matrix that describes the probability of two specified wind directions following in succession.

This study is concerned with an analysis of the wind field over Liverpool Bay (Fig. 1) in the eastern Irish Sea, and a derivation of the wind direction transition matrix (Stolzenbach et al., 1977; Spaulding et al., 1996) from which a stochastic wind time series was created. The two sets of winds (deterministic and stochastic) were then used in a series of oil spill simulations in which the quantity of oil reaching the shoreline and the transit time for the oil to arrive at the coast were determined. Similar calculations were also made using deterministic winds from a site in the Celtic Sea, and by using a classical wind rose description of the wind in Liverpool Bay plus a wind rose taken from the literature for a site on the Isle of Man in the central Irish Sea. While the use of a direction transition matrix for the derivation of a stochastic wind series, and the weakness of the wind rose approach, is established within the oil spill community, the details of the technique have not been published in the open literature. In consequence, one purpose of the present study is to draw the methodology to the attention of coastal oceanographers.

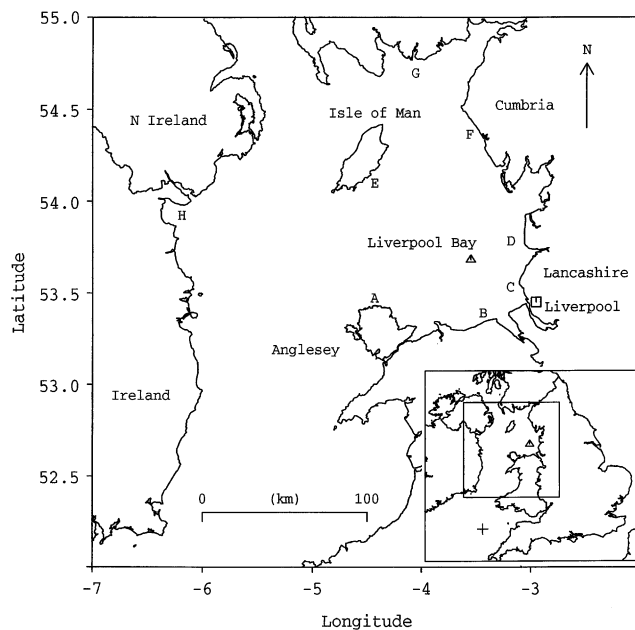


Fig. 1. The Irish Sea showing the location of Liverpool Bay. The simulated release point is marked by a triangle. The inset shows the location of the Celtic Sea wind time series (+).

The spill simulations were made for a hypothetical release location in Liverpool Bay, which lies in the eastern part of the Irish Sea (Fig. 1). Such calculations are not without relevance since there is offshore extraction of both oil and gas in the region. Moreover, the eastern Irish Sea contains a significant number of sites of special scientific interest (SSSIs), special protection areas (SPAs), national nature reserves (NNRs) as well as local nature reserves (LNRs). In addition, there is a proposed marine nature reserve (MNR) in the Menai Strait, which separates the island of Anglesey from the Welsh mainland. Among the issues of special interest in the region is the large number of bird sanctuaries and areas of salt marsh that play a significant role in the passage and wintering of wildfowl.

The tides in Liverpool Bay are predominantly semi-diurnal and have the character of a standing wave so that the maximum currents occur at mid-tide (Bowden, 1980). The spring range at Liverpool is around 10 m, while the tidal currents are strongest off the north coast of Anglesey where they exceed 1.2 m/s at springs (Howarth, 1984). Within Liverpool Bay the tidal streams run generally E–W except for close to the coast where they align with the coastline. The mean flow through the western part of the Irish Sea is weak and has been estimated as having a magnitude of less than 0.01 m/s towards the north (Bowden, 1950). The depth-mean residual flow in Liverpool Bay is driven by winds, density gradients and the residual tidal motion; the weak net circulation showing either a clockwise or anti-clockwise pattern depending on the prevailing large-scale winds. As a consequence of the weak mean flow in the region, the trajectory followed by a surface oil slick depends mainly on the direction of the local winds.

Wind data for the study were taken from an archive of surface winds over the UK shelf seas that were produced by the mesoscale (12 km grid) model of the UK Meteorological Office (Elliott and Jones, 2000). The wind data were available with a time resolution of 6 h and were linearly interpolated spatially to the position of the release point. The wind field was assumed to be spatially uniform over the model domain for the purpose of oil spill simulations. This is a valid assumption as the size of a region influenced by an oil spill is likely to be significantly smaller than the correlation scale of the wind field (Jones, 1999). In addition, the mesoscale model results were used to extract a time series of the winds at a location in the Celtic Sea at a distance of about 300 km from the Liverpool Bay site. (The mesoscale atmospheric model covers the entire NW European shelf seas.)

2. The wind field

Assimilated surface winds from the UK Meteorological Office, which represent the best available synthesis of synoptic observations interpolated in space and time

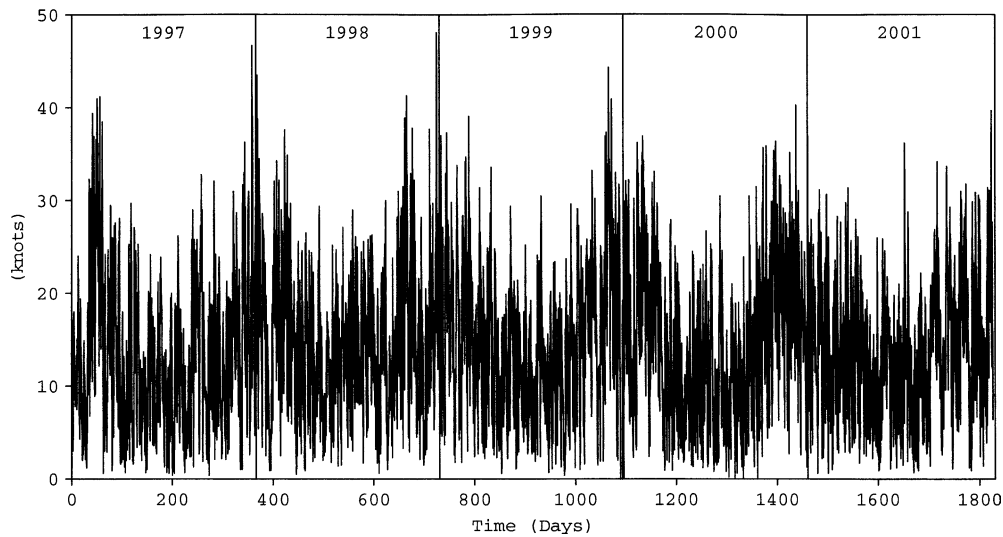


Fig. 2. The Liverpool Bay wind speed (knots) during 1997–2001.

by the 12 km mesoscale model, were available for the years 1997–2001. The data interval was 6 h in 1997–1998 and 3 h from 1999 onwards; the data were therefore uniformly sampled with a time interval of 6 h. Fig. 2 shows a time series of the Liverpool Bay wind speed during 1997–2001. An annual cycle, with increased wind speeds during the winter months, is evident in the data. However, the decrease in wind speed during summer months, which is apparent during 1997 and 2000, is less obvious in 1998, 1999 and 2001. The mean envelope of the maximum wind speed varied from about 20 knots during summer to nearly 50 knots in the winter. However, there were many instances when the summer wind speed exceeded 30 knots. (Although not an SI unit, the knot is commonly used in oil spill simulations. It has therefore been used throughout in the present study. The conversion factor is 1 knot = 0.51 m/s.)

A time scale of around 2–5 days is sometimes referred to in the context of the climate of the UK (Davies et al., 1997) and there is evidence for a periodicity of 2.5–5 days in the wind stress curl and atmospheric pressure records from the Mediterranean region (Elliott, 1979). However, the 2–5 day time scale is a characteristic of weather patterns (e.g. cloudiness and pressure) and may not apply to a time series of wind data, especially at northern latitudes.

A simple estimate of periodicity can be obtained from the zero-up-crossing parameter that is used in the analysis of surface waves (Bowden, 1983, page 98). When applied to the 1997–2001 wind data this provided mean periodicities of 2.8 days and 3.4 days, respectively, for the N–S and E–W components of the wind. The mean value of 3.1 days is in agreement with the expected 2–5 day synoptic time scale. The spectrum of the N–S wind component from Liverpool Bay (Fig. 3) does not show a peak at the synoptic time scale but has a generally

red character; the only significant peak in the spectrum occurs around the 30-day time scale. (A similar result was obtained for the E–W wind component.) However, evidence for spatial structure at the synoptic time scale was provided by the squared coherence derived from a cross-spectral analysis between components of the wind at the Liverpool Bay and Celtic Sea sites which showed significant coherence at time scales longer than 1 day especially around periodicities of 3, 8 and 30 days. It is perhaps not surprising that the wind spectra fail to

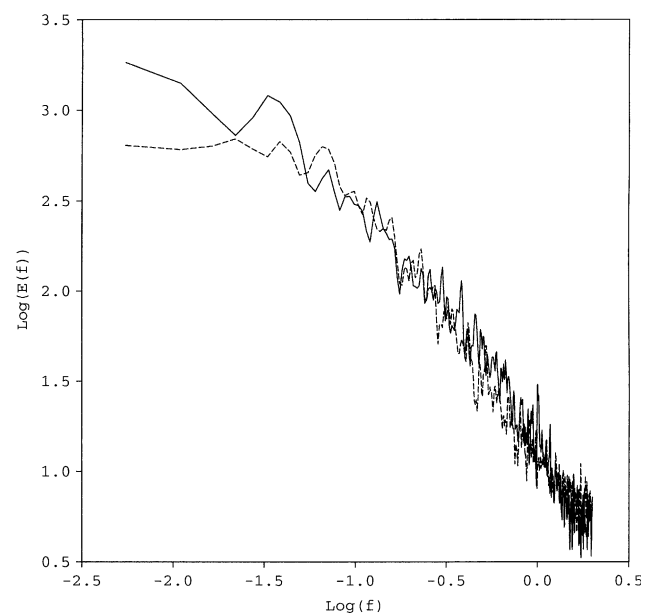


Fig. 3. The energy density spectrum of the N–S component of the 1997–2001 Liverpool Bay wind (solid curve) and the spectrum of the stochastically derived wind (dashed curve). The frequency, f , is expressed in cycles per day and the spectral density, $E(f)$, computed as knots squared per cycles per day.

show an amplitude peak at the synoptic time scale since the method of spectral analysis assumes that the harmonic components are of constant amplitude with fixed phase throughout the entire record length. In contrast the zero-up-crossing period is a robust parameter that makes no assumption about the character of the underlying harmonic components. A zero-up-crossing periodicity of around 3 days was obtained from an analysis of the E–W and N–S components of the wind at both the Liverpool Bay and Celtic Sea sites.

The joint wind speed and direction probability function derived from the 1997–2001 data is presented in Table 1 which contains information equivalent to that provided by a traditional 12 direction sector wind rose. The direction sectors are centred on the given bearings so that, for example, 0° covers the range 345–015°. It is apparent that the most common wind speeds lay in the range 10–15 knots and that the most frequent direction was the sector centred at 240°. This agrees with the expectation that the prevailing winds over the Liverpool Bay region are generally from the SW. For 90% of the time the wind speed was less than 25 knots, while speeds in excess of 35 knots had an occurrence frequency of less than 1%. The most common speed/direction combination was for winds of 15–20 knots from 240°, which

occurred for almost 4% of the time. By integrating separately over direction and speed we can derive the one-dimensional probability functions of wind conditions expressed as functions of speed and direction alone, and these are given below and to the right of the main table, respectively.

Fig. 4 presents the joint probability functions for the individual years from 1997 to 2001 and for the combined years 1997–2001 as direction/speed contour plots. In contrast to the combined years 1997–2001 which showed a most frequent direction of 240°, the years 1998 and 2000 suggested a dominant wind direction from 270° (i.e. a wind from the west) and a most common speed of about 15–20 knots. Moreover, 1997, 1999 and 2001 also showed a tendency for relatively light winds (10–15 knots) to blow from a direction of 120° (i.e. from the SE). Both of these features are reflected in the contour plot for the combined years 1997–2001. It is interesting to compare the annual mean value of the North Atlantic Oscillation index (Jones et al., 2003) with the character of the contour plots shown in Fig. 4. The NAO index averaged from January to December during 1997–2001 gives values of –0.18, 0.26, 0.04, 0.03 and –0.45. Thus the two negative values correspond to the years 1997 and 2001 for which the probability density function plots show the presence of more

Table 1
The joint wind speed and direction probability distribution (expressed as percentages) derived from the 1997–2001 wind data

	Wind speed (knots)											
	0.0	5.0	10.0	15.0	20.0	25.0	30.0	35.0	40.0	45.0	50.0	
330	1.08	1.71	2.04	1.81	0.74	0.16	0.03	0.00	0.00	0.00	0.00	7.57
300	1.12	1.92	2.72	2.41	1.78	0.70	0.23	0.05	0.00	0.00	0.00	10.94
270	1.10	2.27	2.79	3.48	2.57	1.86	0.67	0.18	0.04	0.01	0.01	14.98
240	1.01	1.73	3.07	3.97	3.19	1.86	0.79	0.12	0.05	0.01	0.01	15.81
210	0.78	1.96	2.23	2.16	1.48	0.97	0.41	0.11	0.01	0.01	0.01	10.13
180	0.79	1.48	1.46	1.30	0.55	0.22	0.03	0.00	0.00	0.00	0.00	5.83
150	0.85	1.70	2.01	1.99	0.79	0.36	0.07	0.01	0.00	0.00	0.00	7.78
120	0.82	2.14	2.29	1.56	0.70	0.16	0.03	0.00	0.00	0.00	0.00	7.69
90	0.73	1.85	1.64	0.96	0.52	0.18	0.05	0.00	0.00	0.00	0.00	5.93
60	0.82	1.31	1.41	0.68	0.29	0.07	0.01	0.00	0.00	0.00	0.00	4.60
30	0.53	1.18	0.84	0.45	0.15	0.16	0.00	0.00	0.00	0.00	0.00	3.31
0	1.08	1.44	1.37	0.75	0.52	0.10	0.03	0.00	0.00	0.00	0.00	5.28
	10.72	20.67	23.88	21.52	13.28	6.80	2.35	0.48	0.11	0.04		

The cells contain the percentage of time for which the wind lies within each speed and direction band. The bottom row and right hand column show the one-dimensional percentages as functions of wind speed and wind direction, respectively. The wind direction represents the value at the centre of the bin, e.g. the 0° bin covers the direction range 345°–015°.

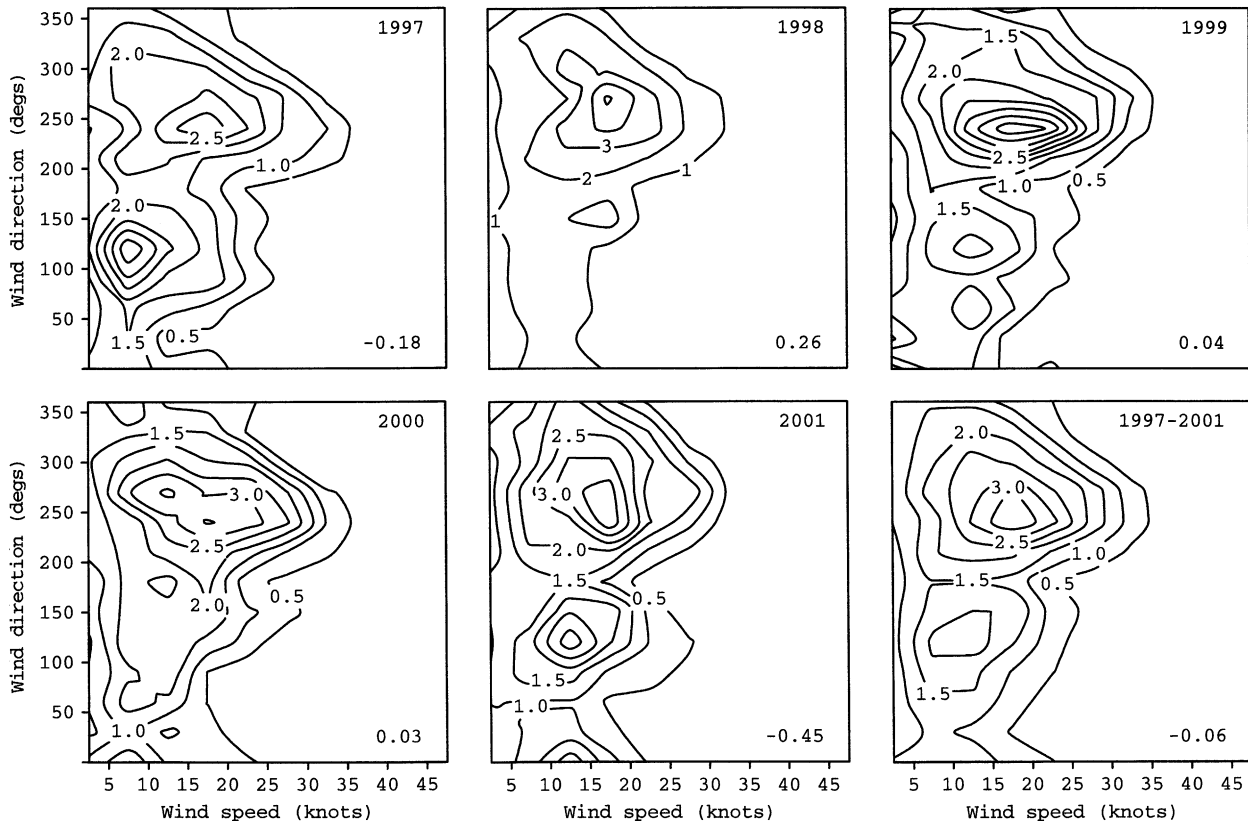


Fig. 4. Joint wind speed and direction probability distributions (expressed as percentages) for Liverpool Bay for the individual years 1997–2001 and 1997–2001 combined. The annual mean value of the North Atlantic Oscillation index is shown near the bottom right corner of each part of the figure.

frequent weak winds from a direction of 120° , while the large positive value for 1998 coincides with the year that shows the lowest frequency of winds from that direction.

The wind direction transition matrix was defined by assigning each of the 6 hourly wind data points to one of the 12 direction bins shown in Table 1. In this manner the time series of wind directions was replaced by a sequence of bin numbers. A wind ‘event’ was thus defined as a sequence of consecutive bin numbers with the same numerical value. The bin sequence was then used to compute the mean duration of a wind event, and the probabilities of consecutive wind directions were derived. This information is presented in Table 2 in which the bins have been related back to the equivalent wind directions. It is apparent that a given wind direction was usually followed by a wind from one of the adjacent sectors. For example, a wind from 180° was followed for 29.5% of the time by a wind from 150° and for 31.6% of the time by a wind from 210° . The mean duration of a sequence of consecutive bin values as defined above, was 10.2 h; however, this should not be interpreted as being equivalent to the zero-up-crossing discussed earlier. If a prevailing wind direction should coincide with the boundary between two adjacent direction bins, the ‘event’ durations for those bins would be shorter than

the true duration as small variations in wind direction would result in a change of the selected bin.

The information contained in Table 2 was then used to create a stochastic wind record that was 5 years long in the following manner:

- An initial wind direction was chosen randomly using the one-dimensional probability function that is given in the column on the right of Table 1.
- For the chosen direction, a wind speed was chosen randomly using the probabilities given in the corresponding row of Table 1. (Note: The direction and speed values were assumed to be distributed linearly within the ranges of the chosen direction and speed bins. They were therefore chosen randomly when the appropriate bins had been selected.)
- The probability p was defined by $p = 1 - \exp(-k\Delta t)$ where k is related to an e-folding time scale, T_e , by $k = 1/T_e$ and Δt is the time step used in a numerical simulation. Then a random number RAN was chosen such that $0 \leq \text{RAN} \leq 1$. The decay process was simulated stochastically by considering the event to have ended if $\text{RAN} \leq p$, otherwise continuing it into the next time step of the simulation (Proctor et al., 1994). Thus a wind direction was

Table 2
The transition matrix for wind direction derived from the 1997–2001 wind data

Wind direction (deg)	330	18.2	4.6	3.0	3.0	4.0	1.3	2.3	4.3	4.0	8.6	46.7	0.0
	300	4.1	1.1	0.5	0.7	2.3	2.5	1.1	3.2	9.7	45.4	0.0	29.6
	270	1.3	0.0	0.5	1.8	1.3	1.4	3.2	9.9	42.4	0.0	30.2	7.9
	240	3.1	0.3	0.5	0.7	3.1	4.1	8.3	32.5	0.0	34.7	10.2	2.4
	210	0.9	0.4	1.3	2.0	4.6	10.6	22.1	0.0	38.4	14.8	3.8	1.1
	180	0.4	0.4	2.5	1.8	4.9	29.5	0.0	31.6	16.1	7.7	3.9	1.4
	150	0.7	2.0	2.6	3.0	26.5	0.0	23.8	20.9	11.9	3.6	4.0	1.0
	120	3.2	5.7	9.2	21.6	0.0	30.7	8.5	5.3	6.7	3.5	3.5	2.1
	90	6.6	6.6	30.1	0.0	39.3	7.7	1.6	1.1	1.1	1.1	2.2	2.7
	60	4.8	27.7	0.0	26.5	18.1	8.4	1.8	3.0	0.0	5.4	1.8	2.4
	30	36.1	0.0	16.7	13.9	10.4	2.8	2.1	4.2	1.4	0.7	2.1	9.7
	0	0.0	21.5	12.4	4.8	2.2	2.2	1.1	0.5	4.8	3.8	8.1	38.7
		0	30	60	90	120	150	180	210	240	270	300	330

The preceding wind direction is tabulated vertically on the left of the matrix, the probability of the subsequent wind direction, expressed as a percentage, is then tabulated horizontally. The diagonal values are zero as the end of a wind event is defined by the transition to a new wind direction.

considered to persist for as long as $RAN \geq p$ with a new value of RAN being chosen on each time step. A value of T_e equal to 20 h, with Δt equal to 6 h, produced the most realistic spectral level in the simulated winds and resulted in the zero-crossing periodicity and the direction transition matrix of the simulated winds matching most closely those obtained from the archived winds.

- (d) For as long as a given wind direction persisted, a suitable speed value was chosen probabilistically using the information in Table 1.
- (e) If $RAN \leq p$ then the wind direction was changed using the transition information contained in Table 2. The sequence of steps (a)–(e) was repeated.

The method used to randomly select a particular bin was based on a probability distribution function, which was derived from the corresponding probability function by integration. For example, if $p(i)$ is the probability defined as

$$p(i) = \text{Probability [an event in bin } i] \quad (1)$$

and $P(i)$ is the cumulative probability defined as

$$P(i) = \text{Probability [an event in one of the bins 1 to } i] \quad (2)$$

a bin can be chosen randomly to satisfy the underlying statistics if a random number RAN is generated where

$0 \leq RAN \leq 1$. Thus given RAN, a k is selected which satisfies

$$P(k-1) \leq RAN \leq P(k). \quad (3)$$

The method can be extended to deal with a two-dimensional probability function such as the one shown in Table 1 by converting it to an equivalent one-dimensional array.

The 5-year stochastic wind record of wind speed and direction was then analysed in an equivalent manner to the archived data. The zero-up-crossing time scales of east and north components of the wind had a mean value of 2.9 days, which is close to the archived data value of 3.1 days. The spectrum of the N–S component of the stochastic wind is shown by the dashed line in Fig. 3. For time scales of 1–10 days there was a good match between the energy levels of the real and synthetic wind. However, the stochastic wind lacked energy at periods longer than 10 days due to the assumption of the e-folding time scale, T_e , in step (c) above.

Fig. 5 shows a section of the archived and stochastic winds to illustrate the realistic manner in which the variability of the wind field is reproduced by the simulated winds. The joint wind speed and direction probability function and the transition statistics derived from the stochastic wind (equivalent to Tables 1 and 2) agreed closely with the results obtained from the archived winds. The following section describes

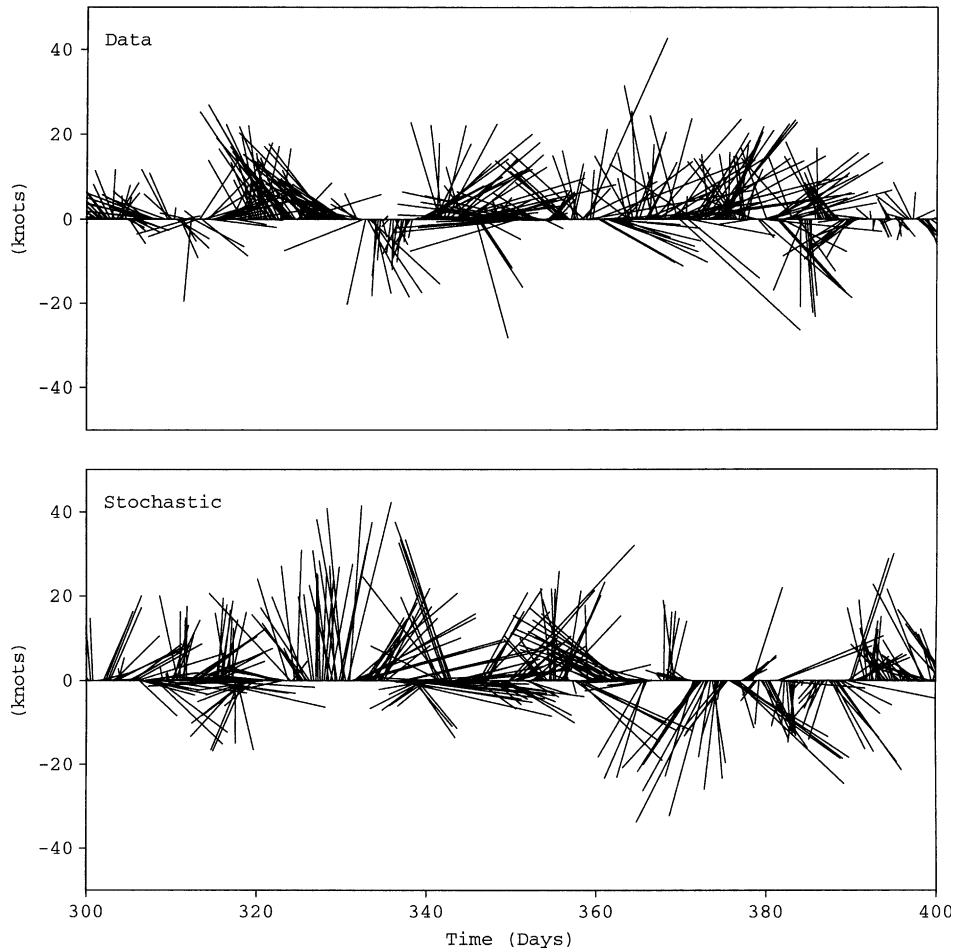


Fig. 5. Vector stick plots showing examples of the archived wind (top) and stochastic wind (bottom).

the use of both real and stochastic winds in oil spill simulations.

3. Spill simulations

A three-dimensional particle-tracking model (Elliott, 1991; Elliott and Jones, 2000) was used to simulate instantaneous releases from the location shown in Fig. 1. Each simulation lasted for 7 days and used values of $10 \text{ m}^2/\text{s}$ for the horizontal diffusivity and $5 \times 10^{-3} \text{ m}^2/\text{s}$ for the vertical diffusivity. The time step used in the calculations was 600 s, the oil droplets were assumed to have a density of $950 \text{ kg}/\text{m}^3$, and the droplet sizes to be in the range 20–500 μm . Particles that reached the shoreline remained fixed to the point at which they beached. The effects of decay and emulsification were not included in the simulations. The model included the M2 and S2 tidal constituents to reproduce the spring/neap character of the tides at the time of the simulation, and also a mean circulation pattern (Elliott et al., 1992). The spill model used a grid with a resolution of approximately 9 km ($1/12^\circ$ of latitude by $1/8^\circ$ of longitude) and these grid cells were used to count the particle density and other

parameters that were derived during the contingency calculations. Model simulations were made using the following sources of wind data.

3.1. Archived winds

For each of these calculations a start time and date were randomly selected from the period 1997 to 2001, 7 days of real winds were then extracted from the archive and used as input data for the model run. During each model run array counters were filled so that the frequency with which individual grid cells were entered by particles and the ‘age’ of particles in each cell could be updated on each time step. Arrays with the accumulated totals were then stored on disk at the end of each model run and aggregated totals were computed following the completion of a sequence of simulations. Winds were used for the position of the Liverpool Bay site and also for the location in the Celtic Sea.

3.2. Wind rose parameterization

The percentages shown for the speed/direction bins of the wind rose derived from the 1997–2001 Liverpool Bay

data (Table 1) were used to weight the probability of selecting a particular combination of wind speed and direction. A bin could then be randomly chosen, and the direction and speed assigned using a uniform probability distribution within the selected direction sector and speed band. This fixed combination of wind speed and direction was then used as input for a spill simulation after choosing a random date and start time. This wind information is equivalent to that which would be provided by a standard wind rose tabulation taken from a climatic atlas. The weakness of this approach is that the speed and direction parameters are held fixed during the simulation, whereas in reality there would be temporal variability in both wind speed and direction. However, the calculations only lasted for 7 days (sometimes significantly less when the dominant wind direction was onshore) and as a consequence the simulation time may not necessarily be long when compared to the typical time scale of the wind events.

3.3. Stochastic wind time series

The 5-year stochastic time series was mapped onto the time interval 1997–2001 and used as a proxy for the real winds. A random start date and time were chosen

and 7 days of consecutive data values were extracted from the time series for each spill simulation.

4. Parameters derived from the simulations

Among the statistical parameters that can be derived from a sequence of spill simulations, the following are of particular relevance:

4.1. The probability of oil entering a grid cell during a release

On each time step of each simulation a flag counter was set to 1 in every grid cell that contained a particle. Once set equal to 1, a flag remained at unity for the remainder of a simulation. At the end of a sequence of N model runs, the cumulative total for each grid cell was computed (say n for a particular cell) and the probability n/N was derived. This statistic therefore represents the probability of a grid cell being impacted by oil during a spill event. For example, Fig. 6 shows the contours of probability derived from 1000 release simulations using winds from the archive and those derived probabilistically by the different methods. At the location of the release the probability is 100% since the release cell

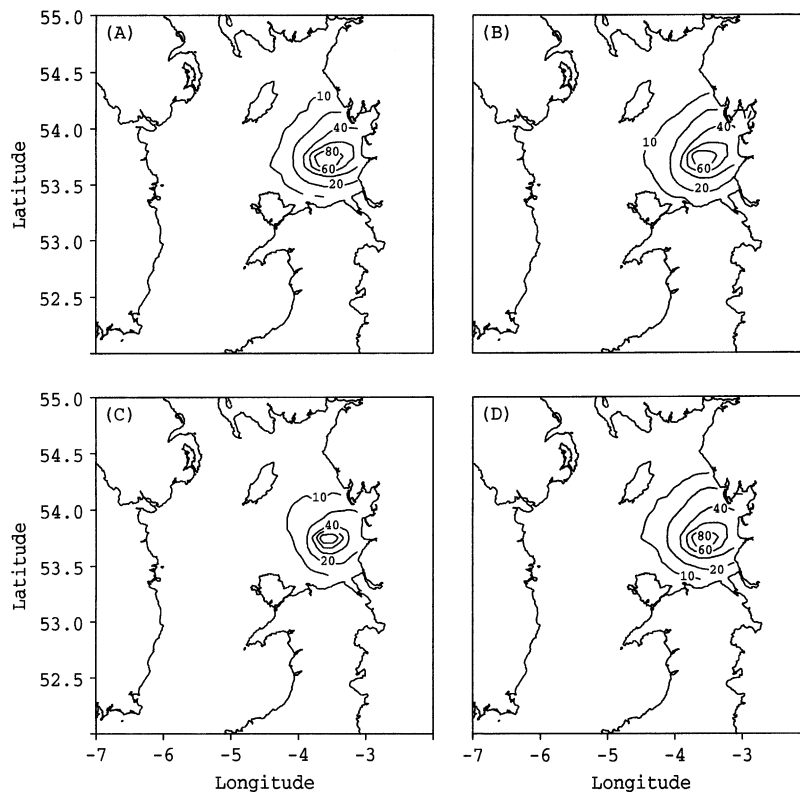


Fig. 6. Contour plots showing the probability (%) of a region being impacted by oil during a spill event: (A) Liverpool Bay wind data, (B) Celtic Sea wind data, (C) Liverpool Bay joint wind speed and direction probability function which is equivalent to a wind rose representation, (D) Liverpool Bay stochastic wind. (The contours are drawn at 10, 20, 40, 60 and 80%.)

contains oil on the first time step of every simulation. In contrast values at the coast to the east of the release point vary between 20 and 50%.

4.2. The exposure of a grid cell to oil during a spill event

The elements of an array were set to 1 each time that a particle entered a grid cell during a model time step and the cumulative total of counts was tabulated during a simulation. The accumulated total within each cell was then computed at the end of a sequence of model runs and was divided by the total summed over all impacted cells. This parameter thus represents the exposure of a grid cell during a typical spill event. The largest values occurred at the coast to the east of the release position where maximum values of 6–8% were obtained.

4.3. The location of oil at the end of each simulation

Arrays were flagged at the end of each simulation (either at the end of 7 days or when all the particles had reached the coast if that occurred sooner) to record the final positions of particles. The probability of oil terminating in each grid cell could then be assessed. The highest values occurred at the coast to the east of the release point where values were typically around 10%; in total about 50% of the oil is likely to beach along the Lancashire coastline. In contrast only about 5% of the oil is likely to beach along the coast of North Wales; moreover, a significant quantity of oil is likely to remain offshore at the end of 7 days. (About 300 of the 682 offshore cells are likely to contain some oil at the end of 7 days. The region shown in Fig. 1 contains 1440 grid cells of which 682 are ‘wet’ cells.)

4.4. The time taken for oil to reach the coast

The time taken for particles to reach coastal cells was stored during each simulation. The aggregate results could then be inspected and the mean and minimum transit times to each coastal grid cell could be computed. As an example, Fig. 7 shows the minimum and mean transit times derived from a sequence of 1000 simulations using the Liverpool Bay archived mesoscale winds. For the Lancashire coastline to the east of the release point the minimum transit times were of the order of 10–15 h. As the release point was located about 30 km offshore, this implies a wind speed of about 20 m/s (40 knots). This is a relatively rare event: winds from 270° in excess of 35 knots only occurred for about 0.2% of the time during 1997–2001 (Table 1). However, the tidal currents in the region are directed E–W and can reach a speed in excess of 1 m/s at spring tides, which would result in a tidal excursion of about 14 km. Thus if a spill happened at the start of a flood tide the oil could reach the coast (where the tidal currents run N–S) in the required time during onshore winds in excess of 25 knots. This wind condition occurs for about 3% of the time (Table 1).

5. Results

Barker and Galt (2000) have derived expressions for the error bars that should be attached to estimates of the quantity of oil that will reach a coastal grid cell following a sequence of numerical simulations. At a more simplistic level, the computational effort for a sequence of trials depends on the product of the number of particles tracked in each simulation and the number of

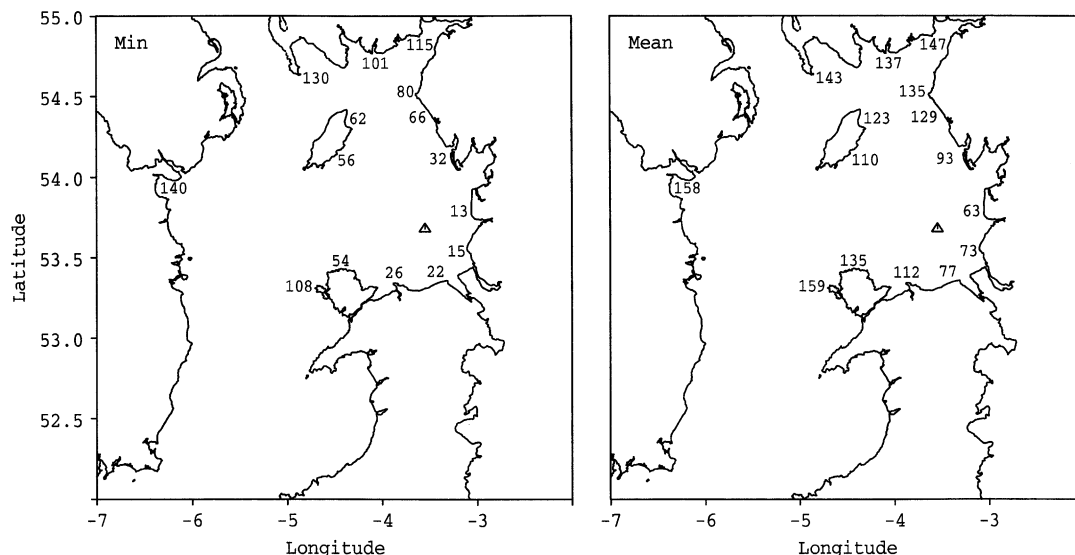


Fig. 7. The minimum and mean time (hours) for oil to reach selected coastal locations. (Results taken from Trial 1.)

releases in each trial. In order to sample the wind field adequately, intuition suggests that, for a given computational effort, it would be better to have a large number of releases with a relatively small number of particles in each release rather than a small number of releases each involving a large number of particles. A trial involving 50 particles and 10,000 simulations required about 10 h of computation on a Unix workstation. In contrast, trials involving 500 particles and 1000 simulations required only 2 h of computation. While in theory these two sets of trials should require similar computational effort, the marked difference in timing arises because the compiler was more efficient at executing arithmetic in comparison to the speed with which it opened and closed input/output files.

With 5 years of wind data available in the wind archive, a trial involving 10,000 simulations would imply a mean separation between the random start times of about 4.4 h. As this interval is significantly less than the characteristic time scale of the wind events, it implies that not all of the trials would be independent. Reducing the number of simulations to 1000 would produce a mean separation of 44 h, which would give a more meaningful resolution of the synoptic time scale. If a time scale 3 of days is considered to be representative of the synoptic time scale, then 600 simulations would be sufficient to adequately sample the archived wind field. Thus 1000 releases will oversample the wind field by a factor of around 2.

5.1. The numerical trials

The 6 numerical trials included:

1. 1000 releases with archived winds from Liverpool Bay.
2. A repeat of (1) to assess the robustness of the statistical results.
3. Similar to (1) but using archived winds from a location in the Celtic Sea approximately 300 km from the spill site.
4. 1000 releases using a 12-sector wind rose derived from the Liverpool Bay archived winds (Table 1).
5. 1000 releases using a 12-sector wind rose for the Isle of Man taken from the literature (Chandler and Gregory, 1976).
6. 1000 releases using the 5-year long time series of stochastic winds.

Trial 3 used archived winds, derived during a study into the *Sea Empress* oil spill (Elliott and Jones, 2000), taken from a position that is 300 km away from the hypothetical Liverpool Bay spill site. In a study of the sensitivity of spill simulations to wind data, Jones (1999) concluded that the error that would result from assuming that the wind field was spatially uniform over a region of

Table 3

The percentage of oil arriving at the coastal cells A–H, the minimum transit time (hours) and the mean transit time (hours) for the 6 trials

	A	B	C	D	E	F	G	H
1	0.0% 54/135	0.3% 22/77	4.3% 15/73	7.7% 13/63	0.0% 56/110	0.0% 66/129	0.0% 101/137	0.0% 140/158
2	0.0% 45/125	0.3% 23/87	4.3% 15/69	8.7% 13/62	0.0% 53/108	0.0% 61/116	0.0% 96/133	0.0% 127/138
3	0.0% 44/114	0.7% 17/77	3.3% 15/67	8.0% 13/66	0.0% 66/124	0.3% 47/102	0.0% 80/124	0.0% 151/162
4	0.0% 53/123	1.0% 16/88	4.7% 13/58	6.7% 13/53	0.0% 47/107	0.0% 43/99	0.0% 80/127	0.0% 136/157
5	0.0% 40/101	1.3% 20/92	3.3% 16/65	4.3% 13/58	0.3% 31/79	0.0% 29/96	0.0% 57/108	0.0% 86/130
6	0.0% 40/117	0.7% 14/83	4.7% 15/69	7.3% 13/66	0.0% 52/118	0.3% 51/116	0.0% 98/128	0.0% 140/145

Trials: 1—Liverpool Bay time series; 2—repeat of Trial 1; 3—Celtic Sea time series; 4—Liverpool Bay wind rose; 5—Isle of Man wind rose; 6—stochastic wind series.

order 100 km × 100 km would be less significant than the errors due to the inaccuracy of the forecast winds at a single point. Thus the purpose of Trial 3 was to evaluate the use of a non-local wind series. The results from Trial 1 were used as the benchmark against which the results from the other simulations could be compared.

5.2. The coastal target locations

Table 3 presents the results for 8 selected coastal cells in Liverpool Bay and other parts of the northern Irish Sea. The 8 coastal regions, A–H, are shown in Fig. 1. Table 3 shows the percentage of oil impacting the cell, the minimum beaching time and the mean transit time to the shore in hours. Estimates for each of the 8 locations were derived by averaging the results from 3 adjacent coastal cells along the coast centred on the target site.

5.3. Numerical results

The results shown in Table 3 suggest that of the 8 selected sites, only C and D to the east of the release point are likely to be significantly affected by oil. At these two sites the results from Trial 1 suggested that 4–8% of the oil was likely to impact the coastal grid cells, with mean transit times of about 60–70 h, and minimum transit times of around 14 h. Trial 2 produced similar statistics, which suggests that the results derived from 1000 random releases are relatively robust. However, care must be taken when considering the results shown in Table 3 as only locations C and D received significant numbers of tracked particles from which reliable statistics can be derived. For the other locations the numbers of received particles were relatively small and

less confidence can be attached to the results—even though each row of the table is based on 1000 simulations involving 500 tracked particles.

The mean time for oil to reach the Isle of Man (location E) was estimated to be about 110 h, with a minimum likely transit time of about 55 h. Locations in the northern and western parts of the Irish Sea (sites G and H) would be impacted on average about 130–150 h after an incident, with minimum transit times of around 90–130 h (Fig. 7). Overall, the results suggest that around 25% of the released oil would impact the Lancashire coastline directly to the east of the spill site. The largest percentage difference between Trials 1 and 2 were obtained for coastal site A (north Anglesey) where the errors in the minimum transit time were about 20%. This probably reflects the infrequency with which winds blow from the NE.

Broadly comparable estimates of the percentage of oil that would reach the coast were obtained when the wind data were taken from an archive that was developed for a location in the Celtic Sea, 300 km to the SW of the hypothetical spill site (Table 3, Trial 3). Moreover, the transit times were similar to those obtained using the local winds for sites B, C and D.

The use of a 12-sector wind rose derived from the 1997–2001 Liverpool Bay wind archive was used in Trial 4. While the percentage of oil likely to impact the coastline to the east of the spill site was comparable to the previous estimates, the mean transit times were significantly lower. For example, at both the sites C and D the mean transit times reduced by about 10–15 h with respect to those obtained in Trial 1. Thus the use of a time invariant wind reduced the mean transit time but had little impact on the minimum time taken for oil to reach the shore, which remained at about 13 h.

However, the agreement was less convincing when a 12-sector wind rose based on data from the Isle of Man covering the years 1957–1971 was taken from the literature (Chandler and Gregory, 1976). The results derived from the use of that wind rose (Table 3, Trial 5) suggested that more than 1% of the oil could impact the beaches of North Wales at site B while only 3–4% would arrive at cells C and D at the Lancashire coast. These results also suggested that oil would be likely to move more towards the south rather than towards the east as shown by the other simulations. However, it is difficult to discern if this is due to the use of winds from an island location as opposed to an open water site or whether it reflects a real change in the wind climate between the periods 1957–1971 and 1997–2001.

The results obtained by the use of the stochastic wind series (Trial 6 in Table 3) agreed well with those obtained when using archived winds (Trials 1–3). The percentage of the oil arriving at the heavily impacted sites, C and D, and the minimum and mean transit times showed better agreement with the benchmark test than

those that were obtained by using a wind rose representation of the wind (Trials 4 and 5).

6. Summary and conclusions

A 5-year long time series of the surface wind at a location in Liverpool Bay was extracted from the output of the UK Meteorological Office 12 km mesoscale model. The assimilated forecast winds were interpolated spatially to the study position and sampled every 6 h. A characteristic time scale of 3.1 days was derived from the data using the method of zero-up-crossing analysis. The spectra of the wind components were red in character and failed to show a peak at the synoptic (2–5 day) time scale. The joint wind speed and direction probability function (Table 1) derived from the data showed that the most common wind speeds lay in the range 10–15 knots and were from a direction of 240°. The NAO index, averaged from January to December of each year, suggested that there is a dependence of the character of the winds over Liverpool Bay on the large-scale pressure distribution (Fig. 4).

A wind direction transition matrix (Table 2) was derived from the 5-year wind time series and used with an estimate of the characteristic time scale to derive a stochastic wind time series. This time series matched the original data in terms of its energy level at the 1–10 day time scale, its persistence and its directional variability. Three classes of wind data: archived values, fixed wind speed and direction estimates derived from a wind rose, and the stochastically created winds were then used with an oil spill model to study the sensitivity of the results to the input wind data.

Fig. 6 shows one of the main results from the oil spill contingency calculations. The simulations made using the archived winds from Liverpool Bay (Fig. 6A) were broadly reproduced when winds were used from a site 300 km away in the Celtic Sea (Fig. 6B). Thus the analysis of Jones (1999), which showed that the spatial variability in winds over a scale of order 100 km was likely to be less than the errors in the forecast at a chosen site, can be extended by stating that over scales of up to 300 km there is spatial coherency in the spatial structure of assimilated winds. This conclusion was supported by computing the cross-spectrum of wind components taken from the Liverpool Bay and Celtic Sea archives; the winds from the two sites were coherent at time scales longer than 1 day, with statistically significant peaks at periodicities near 3, 8 and 30 days.

In contrast to the results obtained using archived data, the simulations provided by a wind rose parameterization of the winds (Fig. 6C) failed to reproduce fully the onshore transport, which therefore resulted in an apparent reduced impact of the oil. This can be explained as a consequence of the fixed value of wind

speed and direction that was used in each of the simulations. The fixed values would cause the oil to move in a generally straight line from the release point towards the eventual beaching location. (There would be some variability in the trajectory due to the influence of the tidal motion and the effects of horizontal diffusion.) In contrast, the archived winds would fluctuate in both speed and direction during each simulation, which would cause a single parcel of oil to move through a much larger number of grid cells before arriving at the shoreline. Thus the area impacted by oil is larger and more diffuse in Fig. 6A and 6B when compared with the results shown in Fig. 6C. The results obtained through the use of stochastic winds, generated using knowledge of the wind direction transition matrix, produced results (Fig. 6D) that agreed well with those obtained from the simulations that used archived winds. It is particularly encouraging that the results shown in Fig. 6A and 6D agree well, as this provides a validation that the stochastic winds are a faithful statistical proxy of the real data from which they were derived.

Estimates were made of the exposure (%) of grid cells to oil, a parameter that sums to 100% when integrated over the entire model domain. In the benchmark calculations made using the Liverpool Bay archived wind time series, the exposure reached values in excess of 6% at the coastal cells to the east of the release point. However, the wind rose simulations resulted in shoreline values of around 4% at similar locations. In contrast, the use of stochastic winds resulted in values of 5–6%. Both the sets of results, therefore, show that the stochastic winds are a better representation of real winds than a parameterization based on a wind rose tabulation.

The use of winds derived from a wind rose produced estimates of the mean time taken for oil to reach the coast that were shorter than the times derived when using archived winds (Table 3). This is a consequence of the time invariant winds used in the wind rose method. Another consequence of the use of wind rose data was an increase in the exposure to oil of grid cells near the spill site. This probably reflects the relatively high frequency with which light winds occur since, as shown by Table 1, wind speeds of less than 5 knots occurred for about 10% of the time.

When available, the use of data from a wind archive or from a wind field derived by an operational atmospheric model (e.g. Reed et al., 1999) is preferable to the use of wind statistics taken from a wind rose. The Liverpool Bay simulations were made using a 5 year data series, and a wind rose derived from these data produced rather different results to those that were obtained when the wind was parameterized using a wind rose description of the winds at the Isle of Man from the period 1957 to 1971. The spatial separation of these two locations is probably not the source of the disagreement since Jones (1999) has shown that wind fields in this

region are spatially uniform over scales of the order of 100 km × 100 km, a result that is reinforced by the coherence results obtained between the winds from Liverpool Bay and a site 300 km away in the Celtic Sea. In consequence, therefore, the discrepancy between the Liverpool Bay and Isle of Man wind roses suggests a change in the wind characteristics between the two periods concerned (1957–1971 and 1997–2001). Finally, the usefulness of climatic summaries would be enhanced if a direction transition matrix was published alongside the conventional wind rose description. Such additional information would allow the creation of a stochastic wind series for use in a range of modelling studies, especially in circumstances when a relatively short wind data set must be used to force an ocean model for a simulation that is longer than the duration of the wind observations.

Acknowledgements

This study was supported by the Chief Scientist's Group of the Department for Environment, Food and Rural Affairs (DEFRA) within contract AE1021, and also by the EU INTERREG IIIA project 'Predictive Irish Sea Models – PRISM'.

References

- Barker, C.H., Galt, J.A., 2000. Analysis of methods used in spill response planning: trajectory analysis planner TAP II. *Spill Science and Technology Bulletin* 6, 145–152.
- Bowden, K.F., 1950. Processes affecting the salinity of the Irish Sea. *Monthly Notice of the Royal Astronomical Society, Geophysical Supplement* 5, 63–90.
- Bowden, K.F., 1980. Physical and dynamical oceanography of the Irish Sea. In: Banner, F.T., Collins, M.B., Massie, K.S. (Eds.), *The North-West European Shelf Sea: the Sea Bed and the Sea in Motion. II Physical and Chemical Oceanography and the Physical Resources*. Elsevier, Amsterdam, pp. 391–413.
- Bowden, K.F., 1983. *Physical Oceanography of Coastal Waters*. Ellis Horwood Limited, Chichester, 302 pp.
- Chandler, T.J., Gregory, S., 1976. *The Climate of the British Isles*. Longman, London, 390 pp.
- Davies, T., Kelly, P.M., Osborn, T., 1997. Explaining the climate of the British Isles. In: Hulme, M., Barrow, E. (Eds.), *Climates of the British Isles*. Routledge, London, pp. 11–32.
- Elliott, A.J., 1979. Low frequency sea level and current fluctuations along the coast of N.W. Italy. *Journal of Geophysical Research* 84, 3752–3760.
- Elliott, A.J., 1991. EUROSPILL: oceanographic processes and NW European shelf databases. *Marine Pollution Bulletin* 22, 548–553.
- Elliott, A.J., Jones, B., 2000. The need for operational forecasting during oil spill response. *Marine Pollution Bulletin* 40, 110–121.
- Elliott, A.J., Dale, A.C., Proctor, R., 1992. Modelling the movement of pollutants in the UK shelf seas. *Marine Pollution Bulletin* 24, 614–619.

- Galt, J.A., Payton, D.L., 1999. Development of quantitative methods for spill response planning: a trajectory analysis planner. *Spill Science and Technology Bulletin* 5, 17–28.
- Howarth, J., 1984. Currents in the eastern Irish Sea. *Oceanography and Marine Biology: an Annual Review* 22, 1–53.
- Jones, B., 1999. The use of numerical weather prediction model output in spill modelling. *Spill Science and Technology Bulletin* 5, 153–159.
- Jones, P.D., Osborn, T.J., Briffa, K.R., 2003. Pressure-based measures of the NAO: a comparison and an assessment of changes in the strength of the NAO and its influence on surface climate parameters. In: Hurrell, J.W., Kushir, Y., Visbeck, M. (Eds.), *North Atlantic Oscillation*. American Geophysical Union, Washington, DC, pp. 51–62.
- Proctor, R., Flather, R.A., Elliott, A.J., 1994. Modelling surface drift in the Arabian Gulf – application to the Gulf oil spill. *Continental Shelf Research* 14, 531–545.
- Reed, M., Ekrol, N., Rye, H., Turner, L., 1999. Oil spill contingency and response (OSCAR) analysis in support of environmental impact assessment offshore Namibia. *Spill Science and Technology Bulletin* 5, 29–38.
- Spaulding, M.L., Opishinki, T., Haynes, S., 1996. COASTMAP: an integrated monitoring and modeling system to support oil spill response. *Spill Science and Technology Bulletin* 3, 149–169.
- Stolzenbach, K.D., Madsen, O.S., Adams, E.E., Pollack, A.M., Cooper, C.K., 1977. A review and evaluation of the basic techniques for predicting the behavior of surface oil slicks. School of Engineering, MIT, Report 222, 315 pp.